2023 IEEE International Conference on Robotics and Automation (ICRA 2023)
May 29 - June 2, 2023. London, UK

Design and characterization of a low mechanical loss, high-resolution wearable strain gauge

Addison Liu, Seun Araromi, Conor J. Walsh, Robert J. Wood
John A. Paulson School of Engineering and Applied Sciences
Harvard University, Cambridge, MA, USA

***Abstract*—Soft, wearable systems hold promise for a wide variety of new or enhanced applications in the realm of human-computer interaction, physiological monitoring, wearable robotics, and a host of other human-centric devices. Soft sensor systems have been developed concurrently in order to allow these wearable systems to respond intelligently with their surroundings. A recently reported sensing mechanism based on the strain-mediated contact in anisotropically resistive structures (SCARS) is an attractive solution due to its high sensing resolution, low-profile nature, and high mechanical resilience. Furthermore, the resistance-based output provides a simple electronic readout, facilitating its use in a wide variety of applications. However, previous iterations of the sensing mechanism have exhibited stress relaxation and hysteretic behaviors that limit the scope of its use. Here, we report an iteration of the SCARS mechanism that uses silicone-based materials with low mechanical loss in order to improve the sensor signal stability and bandwidth. A new fabrication approach is developed which permits the incorporation of a liquid elastomer adhesive layer while also preserving the SCARS sensing functionality. The silicone-based SCARS sensors exhibited fast stress relaxation response (< 1 s) and reduced cyclic drift properties by more than half that of previously reported designs. A physiological monitoring demonstration is presented, validating that the new sensor design is mechanically resilient to such applications and has potential for use in real-world wearable use cases.**

***Index Terms*—Soft Sensors and Actuators; Wearable Robotics.**

I. Introduction

Soft, wearable systems are increasingly sought after due to their mechanical compatibility with the human body, promising safer engagement between machines and people with minimal additional mechanical constraints. These soft systems require sensing to enable them to understand their environment and the motions of the wearer. A recently-developed technology offers an especially promising approach to soft strain detection: the strain-mediated contact in anisotropically resistive structures (SCARS) sensing mechanism quantifies deformation through changes in Ohmic contact [1]. Leveraging electrical junctions within microstructured conductors constructed of layered carbon fiber composite (CFC) material, SCARS is able to sense small changes in deformation with high strain resolution. Its simple electronic readout–electrical resistance being proportional to strain–contrasts the complexity of alternative sensor systems, such as those utilizing capacitive approaches [2], promising higher reliability and accuracy. An in-depth comparison of the SCARS sensing mechanism with other commonly utilized transduction mechanisms is provided in [1]. Applied to the body, the sensor detects strains due to local deformations and muscle bulging. These measurements are correlated to muscle force output [3], [4], leading to wearable applications in muscle performance monitoring (Fig. 1).

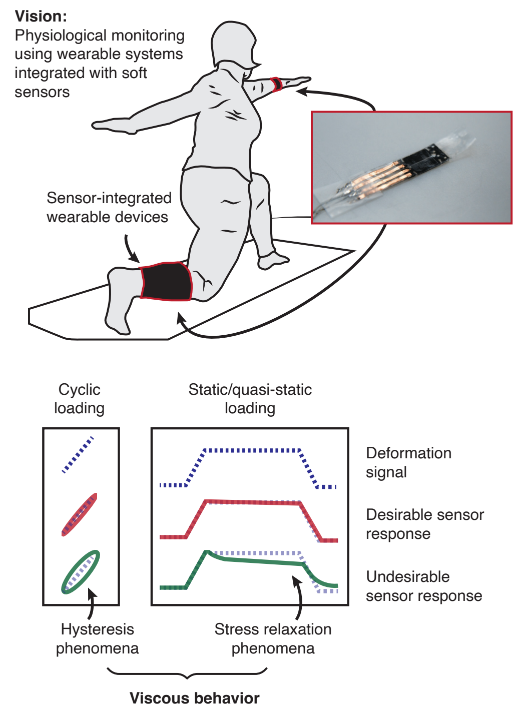

Fig. 1. Wearable system vision. Top: Physiological monitoring of exercise using a wearable device integrated with sensors. Bottom: Schematic of the desired sensor response for a given stimulus, with low viscous behavior (i.e., hysteresis and stress relaxation phenomena) contrasted with an undesirable, prominent viscous behavior.

An ideal strain sensor should possess minimal viscous behavior, e.g., a fast stress relaxation response and low signal hysteresis, enabling high sensing bandwidth and signal stability (Fig. 1). Many soft sensor technologies utilize materials which possess non-negligible viscoelastic properties, leading to viscosity-induced drift and other non-linear phenomena in the sensor response [5], [6]. The SCARS sensor architecture provides flexibility in material selection, allowing for designs that maximize certain aspects of sensor performance, e.g., mechanical robustness, while minimizing others, e.g., flexural rigidity and sensitivity to off-axis loads [1]. However, in order to maximize sensing resolution (the change in electrical response for a given strain), small scale meanders ($<$200 μm) should be utilized. The use of such small features in the sensor design therefore limits the fabrication approaches available and makes the incorporation of low-viscosity materials challenging.

In this work, we develop a strain gauge sensor that builds upon the SCARS mechanism. The sensor operates at strains $<$5% , a range in line with common strain gauge technologies and adequate for quantifying the curvature of physiological surfaces [3]. Previous uses of the SCARS mechanism exhibited stress relaxation and hysteretic behavior [1], limiting its use in applications requiring high bandwidth or long-term signal stability. The new SCARS sensor presented here uses materials with low viscous properties for the encapsulation and adhesive layers, as these are key aspects for optimizing the sensor's mechanical performance. Low-loss materials require the development of a new fabrication method, described here, that is compatible with the SCARS mechanism. Sensors using the new design and fabrication method are characterized and their performance compared against the previously reported designs. We lastly demonstrate the use of the sensor in a proof-of-concept application, namely physiological monitoring of muscle morphology during activation.

II. Sensor Architecture and Fabrication

A. *SCARS architecture*

The SCARS sensing mechanism relies on a five-layer laminate: a micro-structured, rigid conductor, sandwiched between two layers of encapsulation material, held together with an adhesive layer on either side. Mechanically, the micro-structured conductor should display high resilience (e.g., conductor toughness $>$ 10 Nm [1]) and low viscous characteristics. Both the encapsulation material and the adhesive layer should display high elasticity (elastic range $>$ 20%), high tear resilience to survive over-stretching (i.e., deformations beyond the sensing range [1]), and low viscous characteristics (stress relaxation time $<$ 2 s) to preserve signal fidelity and repeatability. Electrically, the encapsulation and adhesive layers should be insulating.

In the initial fabrication approach, CFC was used as the conducting layer, thermoplastic polyurethane (TPU) as the encapsulation layer, and silicone-based pressure-sensitive adhesive (PSA) as the adhesive layer. CFC has a high linear and bending elastic range (being able to sustain large deflections before rupturing) and low viscous properties. A benefit of the SCARS mechanism is that conductors of various thicknesses may be used in sensor construction. Thicker conductors have the advantage of being less susceptible electro-thermal losses (current losses) or damage via melting. The CFC laminate used in this work has an approximate thickness of 150 µm and a trace width of approximately 200 µm, providing a relatively large cross-section area (30×10^{-3}mm^2) to minimize current heating. We hence focus on the encapsulation layers and the adhesive layers–TPU and PSA, respectively–as the domains in which to optimize the viscous properties.

To enhance signal dynamics, we propose replacing the encapsulation and adhesive layers with materials possessing lower viscous properties. In general, silicone elastomers as a class of materials have demonstrated superior viscous properties compared to other stretchable materials such as acrylics and polyurethanes [7]. Therefore, for the encapsulation material, we choose to study (1) a commercially available, prefabricated film (PFF) silicone elastomer (0.2 mm RC0323-FILM, The Rubber Company) for its convenience and uniform film thickness and (2) a two-part silicone elastomer (Sylgard 184, Dow Corning) commonly employed in soft device fabrication [8]. Sylgard 184 is prepared using the manufacturer's recommended mixing ratio of 10:1, silicone base to curing agent, with an automated planetary mixer machine. For the adhesive materials, we choose to study (1) an acrylic-based dry film adhesive (0.5 mil Pyralux® Flame-Retardant Sheet Adhesive, DuPont) and (2) a liquid elastomer adhesive (Sil-poxy, Smooth-On). Used in the fabrication of laminate structures for some millimeter-scale robotic platforms [9], Pyralux possesses a favorable bond strength and its thin-film format is compatible with lab-scale manufacturing processes.

We performed relaxation and cyclic testing on an Instron mechanical tester (model 5544A) to characterize the aforementioned materials, in addition to the materials used in the previously reported sensor for comparison. Stress relaxation properties were quantified using the characterization method from [7] . As illustrated in Fig. 2(a), encapsulation materials were adhered to laser-cut acrylic sample holders with the liquid elastomer adhesive, then bolted to another acrylic holder clasped in a pneumatic grip for testing. As utilized in [7], the normalized stress was plotted against time to facilitate comparison between the different materials. For relaxation testing, samples were rapidly stretched to 10% strain at a rate of 5 mm/s, then held at that strain value for 300 seconds (5 minutes). For cyclic testing, samples were moved through 0-2.5% strain cycles ten times at a constant displacement rate of 4 µm/s to observe hysteric properties (test parameters adapted from [1] and [7]). Relaxation results for encapsulation materials, shown in Fig. 2(b), found that PFF silicone exhibited a stress relaxation response that stabilized (approximately after 1 second) more quickly than the other materials. In contrast, the stress relaxation of the TPU material was still in process by the end of the testing period (300 seconds). The relaxation results for adhesive materials, seen in Fig. 2(c), show that the liquid elastomer adhesive experiences the smallest decrease in mechanical stress and comparable stress stabilization time relative to the other materials investigated. Cyclic testing results for

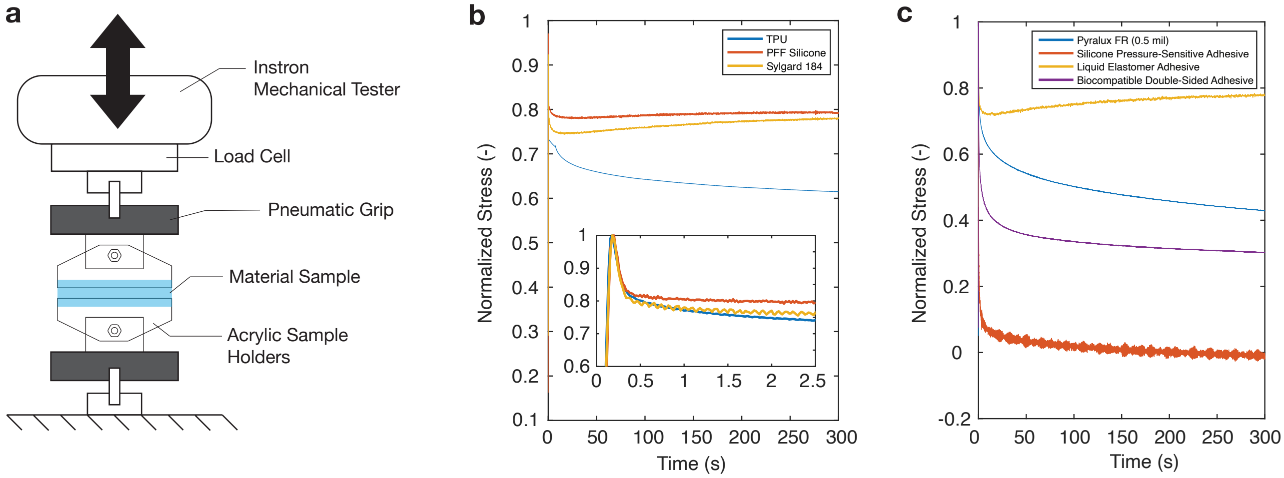

Fig. 2. Materials characterization. (a) Schematic of experimental setup for linear testing. (b) Results for relaxation characterization of encapsulation materials. Inset shows the first five seconds, indicating that PFF silicone stabilizes faster than TPU and Sylgard 184 materials. (c) Results for relaxation characterization of adhesive materials.

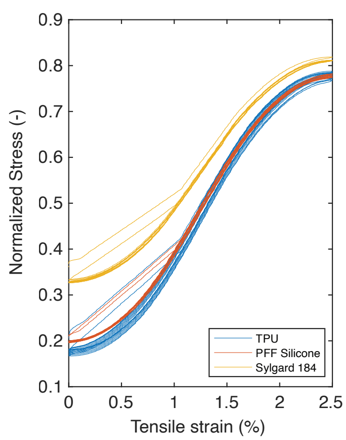

Fig. 3. Results for cyclic characterization of encapsulation materials. PFF silicone exhibits the lowest hysteresis.

encapsulation materials are shown in Fig. 3. Though the hysteresis responses of the materials are qualitatively similar, the PFF silicone exhibits the lowest hysteresis.

Given its stress relaxation response among the materials tested, the PFF commercial silicone is investigated as the sensor encapsulation material. Similarly, the liquid elastomer adhesive is investigated as the adhesive material. The selection of the liquid elastomer adhesive layer necessitates the development of a new fabrication approach. The SCARS mechanism is based on contact between various regions of a micro-structured conductive meander. As a result, the use of liquid adhesives risks covering these contact zones, isolating them electrically and inhibiting the transduction mechanism. We therefore develop a fabrication strategy which is compatible with a liquid adhesive layer, outlined in Fig. 4.

B. Silicone SCARS fabrication process

First, the CFC is functionalized on both sides with polyethylene (PE) film (25 µm thickness), as shown in Fig. 4(a). This functionalization facilitates the bonding of the liquid elastomer material to the surface of the CFC. The PE film layer is incorporated into the CFC layup manufacturing based on the fabrication process outlined in [1]. This layup is placed in a heat press and subjected to heat and pressure, which cures the resin prepregnated in the carbon fiber sheets. Orthogonal stacking minimizes asymmetric stress that would induce curling from heat applied during the curing process. Post-curing, the PE-CFC layup is micro-patterned on the diode-pumped solid-state (DPSS) laser (Fig. 4(b)). The width of the meanders cut into the layup are approximately 200 µm in width, with gaps of approximately 10 µm. These meanders provide geometric stretchability for the CFC conductor. The PE-CFC layup is then cleaned with isopropyl alcohol in an ultrasonic cleaner before the surface is activated via oxygen plasma treatment, further promoting a strong bond between the functionalized CFC surface and the liquid elastomer adhesive (Fig. 4(c)). Immediately following surface activation, the layup is sandwiched between two layers of liquid elastomer adhesive thin film, shown in Fig. 4(d). Minimal pressure is applied during this bonding and curing process to ensure that the liquid elastomer adhesive does not enter the gaps of the meanders. The resulting thin film acts as an adhesion substrate and mechanical barrier, ensuring that the subsequent adhesive layer does not enter the gaps of the CFC meander. Electrical contacts are then added, shown in Fig. 4(e). Here, 1.5 mm strips of copper-coated polyimide films serve as electrical connections to the resistance measurement apparatus; these strips are connected to the PE-CFC layup using a silver conductive epoxy (8331, MG

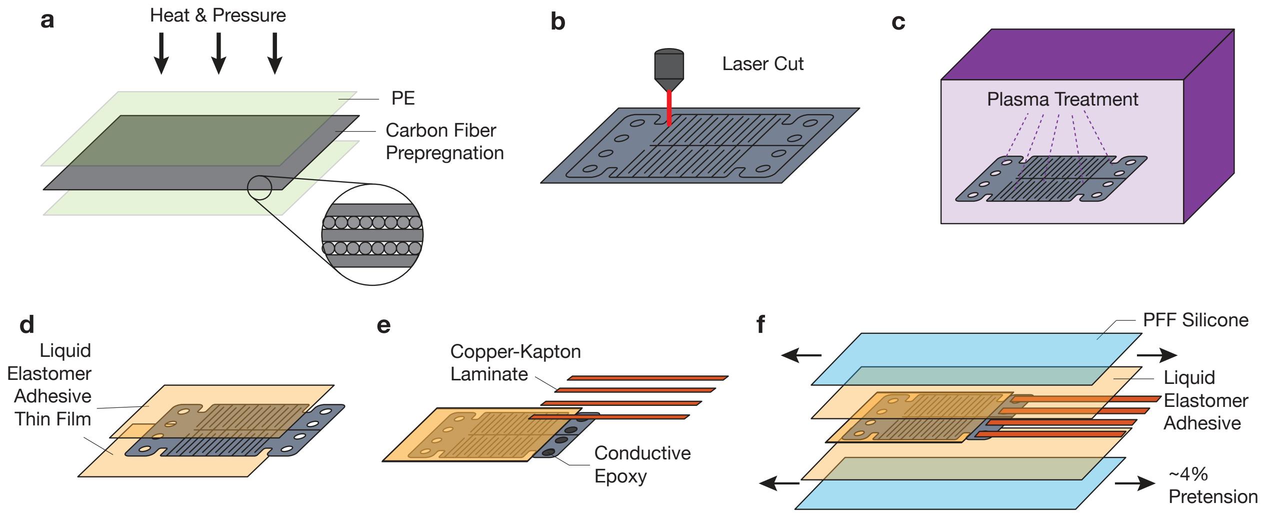

Fig. 4. Silicone SCARS sensor fabrication methodology. (a) Polyethylene (PE)-carbon fiber composite (CFC) layup. CFC consists of five layers arranged orthogonally on top of each other. (b) PE-CFC is patterned on the diode-pumped solid-state (DPSS) laser. (c) Both surfaces of the micro-structured PE-CFC are cleaned and plasma treated. (d) The PE-CFC layup is sandwiched between two layers of 30 μm liquid elastomer adhesive thin film. (e) Electrical connects – strips of copper-coated polyimde film – are adhered to the PE-CFC surface with silver conductive epoxy. (f) The sensor is encapsulated in pre-strained PFF silicone with another thin layer of liquid elastomer adhesive to adhere all layers together.

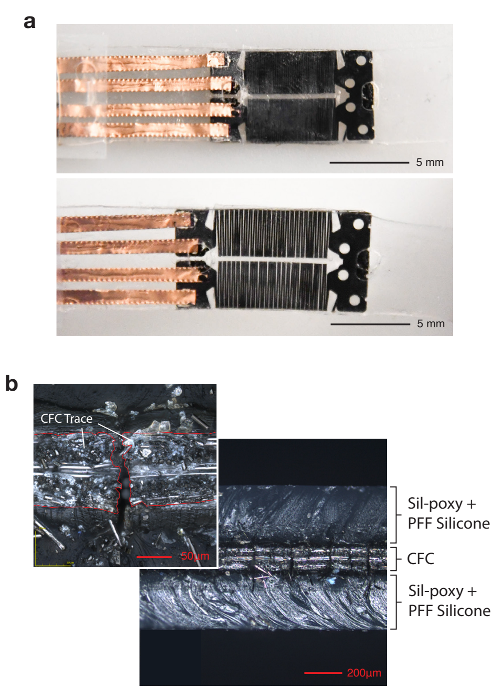

Fig. 5. Silicone SCARS sensors. (a) Sensors in relaxed (top) and stretched states (bottom). Sensor strained beyond its sensing range without damage (b) Cross-section optical microscopy showing the contact zones of the meander and the various layers of the sensor structure.

Chemicals). A four-point resistance measurement approach is used to eliminate the effects of contact resistance and changes in electrical conductivity of the epoxy over time. The entire sensor is then encapsulated with the PFF silicone, which is pre-strained by approximately 4% using acrylic stretching jigs (Fig. 4(f). This pre-strain is necessary to ensure that upon release, adjacent traces come into electrical contact [1]. The PFF silicone is adhered to the sensor with another layer of the liquid elastomer adhesive and left to cure according to manufacturer's instructions. The resulting sensor exhibits a low profile with an overall thickness of 0.75mm and demonstrates stretchability beyond its sensing strain range (sensing range approximately 5%, applied strain approximately 20%) without damage (Fig. 5a).

III. Experimental Characterization

A. Electromechanical characterization

The silicone sensors were tested experimentally to evaluate their electromechanical properties. The responses to both axial strain as well as curvature configurations were demonstrated, representing the two modes of operation previously demonstrated with the SCARS mechanism [1], [3]. In axial strain mode, sensors were secured to acrylic sample holders using bolts, nuts, and cyanoacrylate (CA) glue (Fig. 6(a)). In cyclic testing, samples were moved through 0-10% strain cycles ten times at a constant displacement rate of 83μm/s. In curvature mode, sensors were adhered to a tempered, 125μm-thick sheet steel with CA glue, then mounted to a rigid support on one end (Fig. 7(a)). On the other end, an anvil attached to an Instron mechanical tester moved vertically to deflect the sheet metal, mimicking the bending conditions that may be encountered in wearable applications. The zero position was taken to be where the anvil just contacts the sheet metal in its undeformed, flat state. In relaxation testing, the anvil was displaced 1mm downwards at a rate of 10mm/s

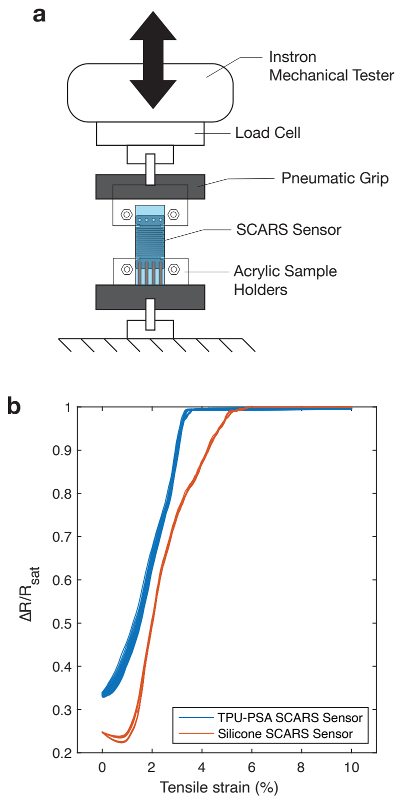

Fig. 6. Sensor characterization in the axial stretching mode. (a) Schematic of the experimental setup for linear testing. (b) Results comparing cyclic characterization of the TPU-PSA SCARS sensor and silicone SCARS sensor.

and held at that displacement for 300 seconds. In cyclic testing, the anvil was moved through 5mm of downward displacement at a rate of 0.4mm/s.

The linear response of the silicone SCARS sensor is comparable to the TPU-PSA architecture previously used [1] , with each sensor having a $R^2 > 70\%$ to a linear fit, as can be seen in Fig. 6. Though silicone elastomers exhibit nonlinear stress-strain behavior (e.g., hyperelasticiy, Mullin's effect etc.), a high linearity in the electromechanical response is achieved because of the small strain range in which the sensor operates. The response to static changes in curvature (Fig. 7(b)) shows that the silicone-based construction exhibits a more stable response with considerably less drift over time (sensor signal stabilized within approximately 2 seconds) than the TPU-PSA construction (sensor signal not stabilized within testing period). Note that both sensors exhibit a small change in signal magnitude during the testing period–less than 6% for the TPU-PSA device and less than 2% for the silicone-based sensor. Cyclic testing of the sensor in curvature mode (Fig. 7(c)) showed that drift in the sensor signal for the TPU-PSA device is notably larger than for the silicone device: the peak sensor value decreased by approximately 3% for the TPU-PSA device compared with less than 1% for the silicone-based sensor.

B. *Physiological monitoring with silicone SCARS sensor*

We demonstrated the efficacy of the silicone-based SCARS sensor with human physiological monitoring in a laboratory setting. As shown in Fig. 8(a), a silicone sensor and a TPU-PSA sensor were placed on the forearm of an adult male participant, approximately on top of the belly of the extensor carpi ulnaris muscle (placement of sensor determined via palpation of the muscle during wrist flexion). The participant gave written consent prior to participating and the protocols are approved by the Harvard Medical School Institutional Review Board under protocol IRB17-1201. The participant was instructed to perform periodic parallel grasping of a force plate instrumented with a load cell. A 2D laser profiler (LJ-X8200, Keyence) was positioned over the silicone set up and used as a ground truth for the sensor deformation during the experiment. The participant's relative force production was tracked via the force plate. The participant was instructed to produce a force and hold it for four seconds (with the assistance of a metronome) and subsequently release the force as quickly as they were able.

The results of the experiment (Fig. 8(b)) show that the sensor response follows the general trend of the force plate signal and laser curvature signal (Spearman's correlation = 0.81). Precise tracking of the force production is challenging given the variety of muscles involved in the movement. However, the results show that the silicone SCARS sensor is as mechanically resilient as its TPU-PSA counterpart for real-world use cases and that the sensor holds promise for applications in physiological monitoring.

IV. Conclusion

A low-loss strain gauge sensor design based on the SCARS mechanism is described in this work. PFF silicone and a liquid elastomer adhesive are studied as low-viscoelastic alternatives to TPU and silicone PSA, used as the encapsulation layer and adhesive layer, respectively, in previous SCARS sensor iterations. A new fabrication process based on the use of PFF silicone and liquid elastomer adhesive is proposed. The result is a low-profile sensor that displays high mechanical resilience and low viscoelasticity. These properties are confirmed by mechanical characterization, which showed an improvement in viscoelastic properties in the new silicone SCARS sensors as compared to TPU-PSA SCARS sensors by more than a factor of 2. The silicone SCARS sensor also demonstrated reasonable signal fidelity in human physiological testing, further proving its potential in wearable sensing systems.

V. Acknowledgements

The authors would like to gratefully acknowledge Diana Wagner for her help with figure preparation, Jonathan Alvarez and Lucas Gerez for their assistance with sensor characterization, the Wyss Institute Clinical Research Team for their help with study protocol development, Arthur Passy

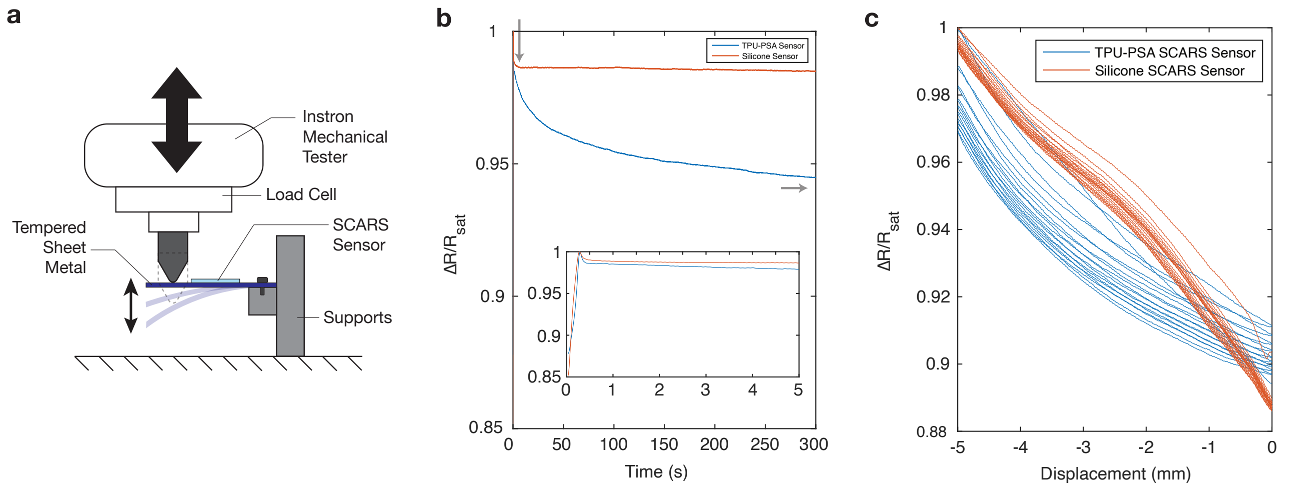

Fig. 7. Sensor response in curvature mode. (a) Schematic of the experimental setup for curvature testing. The SCARS sensor is adhered to tempered sheet metal with cyanoacrylate (CA) glue. (b) Results comparing relaxation characterization of TPU-PSA and silicone SCARS sensors. Arrows indicate stabilization time, where the TPU-PSA sensor does not stabilize within the testing period. (c) Results comparing cyclic characterization of TPU-PSA and silicone SCARS sensors.

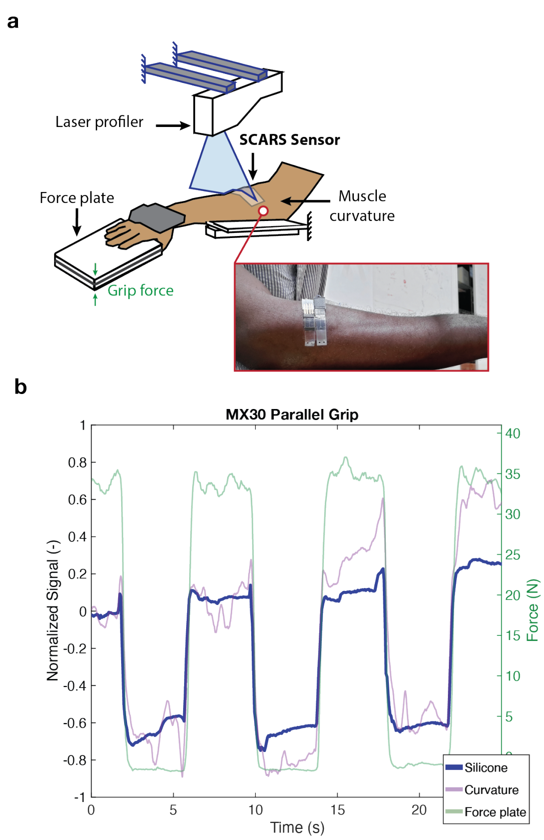

Fig. 8. Real-world demonstration of physiological monitoring. (a) Schematic of experimental set-up demonstrating simultaneous measurement of force produced in wrist flexion and SCARS sensor response placed on the forearm (approximately above the extensor carpi ulnaris muscle). (b) Results of the experiment. Responses of the force plate, silicone SCARS sensor and laser curvature profiler are plotted against time.

for his assistance with physiological monitoring experimental design, Elizabeth Hevia and Lauren Baker for her assistance with manuscript preparation. The work was supported by funding from the Wyss Institute for Biologically Inspired Engineering, by the Aramont Fellowship Fund for Emerging Science Research, and by the Harvard Herchel Smith Undergraduate Fellowship.

REFERENCES

[1] Araromi, O. A., Graule, M. A., Dorsey, K. L., Castellanos, S., Foster, J. R., Hsu, W. H., ... & Wood, R. J. (2020). Ultra-sensitive and resilient compliant strain gauges for soft machines. Nature, 587(7833), 219-224.

[2] Gisby, T. A., O'Brien, B. M., Anderson, I. A. (2013). Self sensing feedback for dielectric elastomer actuators. Applied Physics Letters, 102(19), 193703.

[3] Alvarez, J. T., Gerez, L. F., Araromi, O. A., Hunter, J. G., Choe, D. K., Payne, C. J., Wood, R. J., Walsh, C. J. (2022). Towards Soft Wearable Strain Sensors for Muscle Activity Monitoring. IEEE Transactions on Neural Systems and Rehabilitation Engineering, 30, 2198-2206.

[4] Guo, J. Y., Zheng, Y. P., Xie, H. B., & Chen, X. (2010). Continuous monitoring of electromyography (EMG), mechanomyography (MMG), sonomyography (SMG) and torque output during ramp and step isometric contractions. Medical engineering & physics, 32(9), 1032-1042.

[5] Yuan, J., Zhang, Y., Li, G., Liu, S., Zhu, R. (2022). Printable and Stretchable Conductive Elastomers for Monitoring Dynamic Strain with High Fidelity. Advanced. Functional Materials, 2204878.

[6] Boland, C. S. (2020). Quantifying the contributing factors toward signal fatigue in nanocomposite strain sensors. ACS Applied Polymer Materials, 2(8), 3474-3480.

[7] Michel, S., Zhang, X. Q., Wissler, M., Löwe, C., & Kovacs, G. (2010). A comparison between silicone and acrylic elastomers as dielectric materials in electroactive polymer actuators. Polymer international, 59(3), 391-399.

[8] Johnston, I. D., McCluskey, D. K., Tan, C. K. L., & Tracey, M. C. (2014). Mechanical characterization of bulk Sylgard 184 for microfluidics and microengineering. Journal of Micromechanics and Microengineering, 24(3), 035017.

[9] Sreetharan, P. S., Whitney, J. P., Strauss, M. D., & Wood, R. J. (2012). Monolithic fabrication of millimeter-scale machines. Journal of Micromechanics and Microengineering, 22(5), 055027.